Modification of N^6-methyladenosine RNA methylation on heat shock protein expression

Jiayao Yu, Yi Li, Tian Wang, Xiang Zhong*

College of Animal Science and Technology, Nanjing Agricultural University, Nanjing, Jiangsu, People's Republic of China

* zhongxiang@njau.edu.cn

Abstract

This study was conducted to investigate effect of N^6-methyladenosine (m^{6}A) RNA methylation on Heat shock proteins (HSPs) and dissect the profile of HSP RNA methylation. The results showed that m^{6}A methyltransferases *METTL3* mRNA was decreased in responses to heat shock stress in HepG2 cells, but m^{6}A-specific binding protein YTHDF2 mRNA was upregulated in a manner similar to HSP70 induction. Immunofluorescence staining showed that the majority of YTHDF2 was present in the cytosol, however, nearly all YTHDF2 translocated from the cytosol into the nucleus after heat shock. METTL3 knockdown significantly changed *HSP70*, *HSP60*, and *HSP27* mRNA expression in HepG2 cells using siRNA, however, mRNA lifetime was not impacted. Silence of YTHDF2 using siRNA did not change expression of *HSP70*, but significantly increased *HSP90*, *HSP60*, and *HSPB1* mRNA expression. In addition, m^{6}A-seq revealed that HSP m^{6}A methylation peaks are mainly enriched on exons and around stop codons, and shows a unique distribution profile in the 5'UTR and 3'UTR. Knockdown of METTL3 changed the methylation patterns of HSPs transcript. In conclusion, m^{6}A RNA methylation regulates HSP gene expression. Differential expression of HSPs modulated by m^{6}A may depend on the m^{6}A site and abundance of the target gene. This finding provides insights into new regulatory mechanisms of HSPs in normal and stress situations.

Introduction

Heat shock proteins (HSPs), which are expressed constitutively in all species, are molecular chaperones that regulate protein localization, accumulation, and degradation, assist in protein re-folding, prevent protein aggregation [1], and play important physiological roles in normal conditions as well as situations involving both systemic and cellular stress [2, 3]. Based on their molecular sizes, HSP proteins are classified into a number of conserved protein families, including HSP90, HSP70, HSP60 and small HSPs [4]. It is well known that increase of HSP genes are activated at the transcriptional level by heat shock transcription factor 1 (HSF1) [5]. Interestingly, growing evidence indicates that the expression of HSPs can be attributed to epigenetic changes including DNA methylation and acetylation of histones [6–9]. However, modulation of HSPs expression by RNA methylation remains unclear.

To date more than 100 diverse chemical modifications of RNA have been identified. N^6-methyladenosine (m⁶A) is the most abundant internal modification of eukaryotic mRNA, influencing metabolism and function of mRNAs [10]. M⁶A RNA modifications are dynamically and reversibly regulated by methyltransferases including METTL3 and METTL14 [11], and demethylases including ALKBH5 and FTO [12]. Their functions are exerted by direct recognition by m⁶A-specific binding proteins including YTHDF1 and YTHDF2 [13, 14]. M⁶A shows the most enrichment in translation start sites, stop codons, and 3'UTRs [15, 16], suggesting that it plays important roles in mRNA biology. Indeed, modification of m⁶A on mRNA functionally regulates mRNA splicing [15, 17], export [18], localization, translation [19], and stability [13], suggesting that m⁶A RNA methylation is an epitranscriptomic mechanism that regulates gene expression.

The precise sites and abundance of m⁶A are highly regulated under normal conditions, however, previous reports showed that cellular stress, such as heat shock or ultraviolet radiation, alters characteristic distribution and function of m⁶A [15, 20]. This finding suggests that changes of m⁶A may contribute to tuning a number of genes expressed under stress conditions. Indeed, Zhou et al. [21] found that m⁶A modification altered by heat shock stress and activate Hsp70 mRNA translation. However, manipulation of m⁶A RNA methylation on other stress-inducible chaperones such as HSP90, HSP60, and HSP27 remain unknown.

Here, we investigated the topology and function of m⁶A modifications of HSPs RNA, including *HSPA1B*, *HSPA9*, *HSP90AA1*, *HSPD1*, *HSF1*, and HSPB1 using m⁶A-seq in HepG2 cells.

Materials and methods

All the procedures were approved by the Institutional Animal Care and Use Committee of Nanjing Agricultural University, China.

Cell lines

The human HepG2 cell line used in this study was obtained from the American Type Culture Collection (ATCC) at passage 5 and grown in DMEM (Gibco, Grand Island, NY, USA) media supplemented with 10% FBS, and 1% 100× Pen Strep. HepG2 cells were incubated with 5% CO_2 and 95% air at 37˚C.

Heat shock

HepG2 cells were subjected to 41˚C heat shock in a water bath for 1 h and then recovery incubation at 37˚C The cells were harvested at 6 h, 12 h, 24 h after heat shock and processed for RT-PCR analysis.

siRNA knockdown

Human *METTL3* and *YTHDF2* siRNAs were ordered from Qiagen (Hs-METTL3 with target sequence CTGCAAGTATGTTCACTATGA, Hs-YTHDF2 with target sequence AAGGACGTTCC CAATAGCCAA). Control siRNA is from Qiagen (1027281). Each siRNA was transfected into HepG2 cells using Lipofectamine RNAiMAX (Invitrogen) for siRNA following the manufacture's protocols. At 48 h after the transfection, cells were harvested and stored at -80˚C for further studies.

RNA isolation and purification

Total RNA was isolated from HepG2 cells using TRIzol (Invitrogen), and contaminant DNA was removed using DNaseI. The RNA integrity was determined on 1% agarose gel with ethidium bromide staining. The concentrations of RNA were quantified by absorbance at 260 nm and 280 nm using a NanoDrop ND-1000 UV spectrophotometer. Messenger RNA for LC-MS/MS was extracted using PolyATtract® mRNA Isolation System III (Promega) followed by further removal of contaminated rRNA by using the Ribominus eukaryote kit v2 (Life technologies).

qRT-PCR

One μg of total RNA was used to synthesize cDNA in a 20 μL reaction mixture using HiScript ®II Q RT SuperMix for qPCR (+gDNA wiper) (Vazyme, Nanjing, China) according to the manufacturer's instructions. Real-time PCR was carried out on the ABI StepOnePlus™ Real-Time PCR systems. Gene-specific primer sequences of the reference and target genes are listed in Table 1 and were synthesized by Invitrogen Biotech Co. Ltd. (Shanghai, China). The following thermal profile was used for qRT-PCR: 95˚C for 3 min, followed by 40 cycles of 95˚C for 10 sec and 60˚C for 30 sec. The relative gene expression was calculated using the $2^{-\Delta\Delta CT}$ method. Both GAPDH and HPRT1 genes were used to normalize variations in the amount of starting material.

Table 1. Primer sequences used in quantitative real time PCR assays.

Gene	Accession No.	Primer, 5'-3'
HSPA1B	NM_005345.5	Sense: GCGAGGCGGACAAGAAGAA Antisense:GATGGGGTTACACACCTGCT
HSPA9	NM_004134.6	Sense: GGAAGGTAAACAAGCAAAGGTGC Antisense:CCAACAAGTCGCTCACCATCT
HSP90AA1	NM_005348.3	Sense: GCTTGACCAATGACTGGGAAG Antisense:AGCTCCTCACAGTTATCCATGA
HSPD1	NM_002156.4	Sense: CTACTGTACTGGCACGCTCTA Antisense:CAACAGCTAACATCACACCTCTC
HSF1	NM_005526.3	Sense: CCATGAAGCATGAGAATGAGGC Antisense:CTTGTTGACGACTTTCTGTTGC
HSPB1	NM_001540.4	Sense: TGGACCCCACCCAAGTTTC Antisense:CGGCAGTCTCATCGGATTTT
METTL3	NM_019852.4	Sense: CAAGCTGCACTTCAGACGAA Antisense: GCTTGGCGTGTGGTCTTT
METTL14	NM_020961.3	Sense: AGAAACTTGCAGGGCTTCCT Antisense: TCTTCTTCATATGGCAAATTTTCTT
FTO	NM_001080432.2	Sense: ACTTGGCTCCCTTATCTGACC Antisense: GTGCAGTGTGAGAAAGGCTT
YTHDF2	NM_001172828.1	Sense: CCTTAGGTGGAGCCATGATTG Antisense: TCTGTGCTACCCAACTTCAGT
GAPDH	NM_001289746.1	Sense: CGACCACTTTGTCAAGCTCA Antisense: AGGGGAGATTCAGTGTGGTG
HPRT1	NM_000194.2	Sense: TGACACTGGCAAAACAATGCA Antisense: GGTCCTTTTCACCAGCAAGCT

HSPA1B heat shock protein 70; *HSPA9* heat shock protein 70; *HSP90AA1* heat shock protein 90; *HSPD1* heat shock protein 60; *HSF1* heat shock factor 1; *HSPB1* heat shock protein 27; *METTL3* methyltransferase like 3; *METTL14* methyltransferase like 14; *FTO* fat mass and obesity associated; *YTHDF2* YTH domain family 2, *GAPDH* glyceraldehyde-3-phosphate dehydrogenase, *HPRT1* hypoxanthine phosphoribosyltransferase 1.

Cell proliferation and viability assay

Cell proliferation was performed using the 3-(4,5-dimethylthiazol-2-yl)-2,5-diphenyltetrazo-lium bromide (MTT) assay according to the manufacturer's instructions (Roche Applied Science). The transfected cells were plated in 96-well plates (3000 cells/well). Cell proliferation was determined at 24 h, 48 h, and 72 h after the transfection or heat shock, respectively.

mRNA lifetime

METTL3 siRNA was transfected into HepG2 cells at 70–80% confluence in 24-well plates using Lipofectamine RNAiMAX (Invitrogen) following the manufacture's protocols. After 48 h transfection, the cells were treated with actinomycin (5 µg/ml) for 6 h, 3 h, and 0 h before trypsinization and collection.

The total RNA was isolated using TRIzol. After reverse transcription, mRNA levels of transcripts of interest were detected by qRT-PCR. The degradation rate of RNA k was estimated by

$$\log_2\left(\frac{At}{A0}\right) = -kt$$

where t is transcription inhibition time (h), A_t and A_0 represent mRNA quantity at time t and time 0. Two k values were calculated: time 3 h versus time 0 h, and time 6 h versus time 0 h. The final lifetime was calculated by using the average of $k_{3\,h}$ and $k_{6\,h}$.

$$t\frac{1}{2} = \frac{2\ln2}{k3h + k6\,h}$$

Immunofluorescence staining

HepG2 cells grown on glass coverslips were fixed in 4% paraformaldehyde in phosphate-buffered saline (PBS) for 10 min at 4˚C, and then were permeated with 0.1% Trition X-100 in PBS for 15 min. Dako blocking solution (Dakocytomation protein block serum-free) was used to block the nonspecific binding of antibodies for 30–60 min. The cells were then incubated with rabbit polyclonal anti-YTHDF2 (Proteintech, 24744-1-AP) diluted in Dakocytomation antibody diluents for 2 h at room temperature or overnight at 4˚C followed by 1 h incubation at room temperature with the secondary Alexa series fluorescently labeled antibodies (1:1500 dilution). After washing with PBST for three times, prolong Gold antifade reagent with DAPI staining was used for nuclei detection (Life Technologies). Confocal microscopy images were captured by Leica SP5 II STED-CW Super-resolution Laser Scanning Confocal instrument and analysed by ImageJ software.

Immunoblotting

Total cellular protein was isolated from HepG2 cells using Cell Lysis Buffer containing Complete Protease Inhibitor (Roche) and PMSF for determination of METTL3. The protein concentrations were determined using the BCA protein assay kit according to the protocol provided by the manufacturer (Nanjing Jiancheng Bioengineering Institue, Jiangsu, China). A total of 20 µg of protein with loading buffer was boiled for 5 min and electrophoretically resolved by 10% reducing SDS-PAGE gels. Protein was then transferred to nitrocellulose membranes. The membranes were blocked for 1 h in TBS containing 5% non-fat milk and 0.1% Tween-20, followed by incubation with mouse polyclonal anti-METTL3 (Novus, H00056339) or mouse monoclonal anti-GAPDH (Invitrogen, MA5-15738-HRP) antibodies

overnight at 4˚C. After incubation with horseradish-peroxidase-coupled secondary antibodies at room temperature for 1 h, immunoblots were visualized using enhanced chemiluminescence (ECL^{Plus})

m^{6}A-seq

For m^{6}A immunoprecipitation, the procedure was modified from the previously reported methods [15]. In brief, total RNA was extracted using TRIzol reagent followed by purification using PolyATtract$^®$ mRNA Isolation System III (Promega). Subsequently, purified mRNAs were digested using DNase I and then fragmented into roughly 100-nt fragments by incubation for 15 min at 70˚C in fragmentation buffer (10 mM Tris-HCl, pH 7.0, 10 mM ZnCl$_2$). 500 ng mRNA was saved as input control for RNA-seq. Five µg fragmented mRNA was incubated with 12 µg anti-m^{6}A antibody (Synaptic Systems) in $1 \times$ IP buffer (10 mM Tris-HCl, pH 7.4, 150 mM NaCl, and 0.1% Igepal CA-630) for 2 h at 4˚C. At the same time, recombinant protein A bead (Invitrogen) was washed twice followed by incubation in $1 \times$ IP buffer with 0.5 mg/ml BSA on a rotating wheel for 2 h at 4˚C. The m^{6}A-IP mixture was then incubated with protein A beads for additional 2 h at 4˚C on a rotating wheel. After washing three times with IP buffer, bound mRNA was eluted using 100 µl elution buffer (6.7 mM N^6-Methyladenosine-5'-mono-phosphate sodium salt in IP buffer) followed by ethanol and sodium acetate precipitation. Immunoprecipitated RNA fragments and comparable amounts of input were subjected to first-strand cDNA synthesis. Sequencing was performed on Illumina HiSeq2500 according to the manufacuture's instructions.

Statistical analysis

Comparisons between the mean ± SEM of two groups were calculated using Student's unpaired two-tailed t test, performed with SPSS software. The following p values were considered to be statistically significant: p value ≤ 0.05 (*), p value ≤ 0.01 (**).

Results

Heat shock changes *HSP70*, *METTL3* and *YTHDF2* mRNA expression

Compared to control group, the expression of *HSP70* mRNA was increased at 6 h, 12 h, and 24 h after heat shock stress in HepG2 cells ($p < 0.05$) (Fig 1A and 1B). Decrease of *METTL3* mRNA expression was observed at 6 h and 12 h after heat shock stress compared to control ($p < 0.05$) (Fig 1C). Heat shock inhibited the expression of *METTL14* mRNA at 6 h after heat treatment ($p < 0.05$) (Fig 1D). We found that there was no change in *FTO* expression after heat shock stress (Fig 1E). However, the expression of *YTHDF2* mRNA was enhanced at 12 h and 24 h after heat shock stress ($p < 0.05$) (Fig 1F).

Heat shock changes localization of YTHDF2

Surprisingly, we found that the majority of YTHDF2 resided in the cytosol under normal condition, however, under heat shock stress nearly all YTHDF2 translocated into the nucleus from the cytosol (Fig 2).

METTL3 knockdown affects HSPs expression and cell proliferation

In order to determine the role of m^{6}A RNA methylation on the regulation of HSPs, *METTL3* was knockdowned using siRNA. Although METTL14 shows a similar regulation as METTL3, here we only observed *METTL3* knockdown because *METTL3* and *METTL14* form a stable
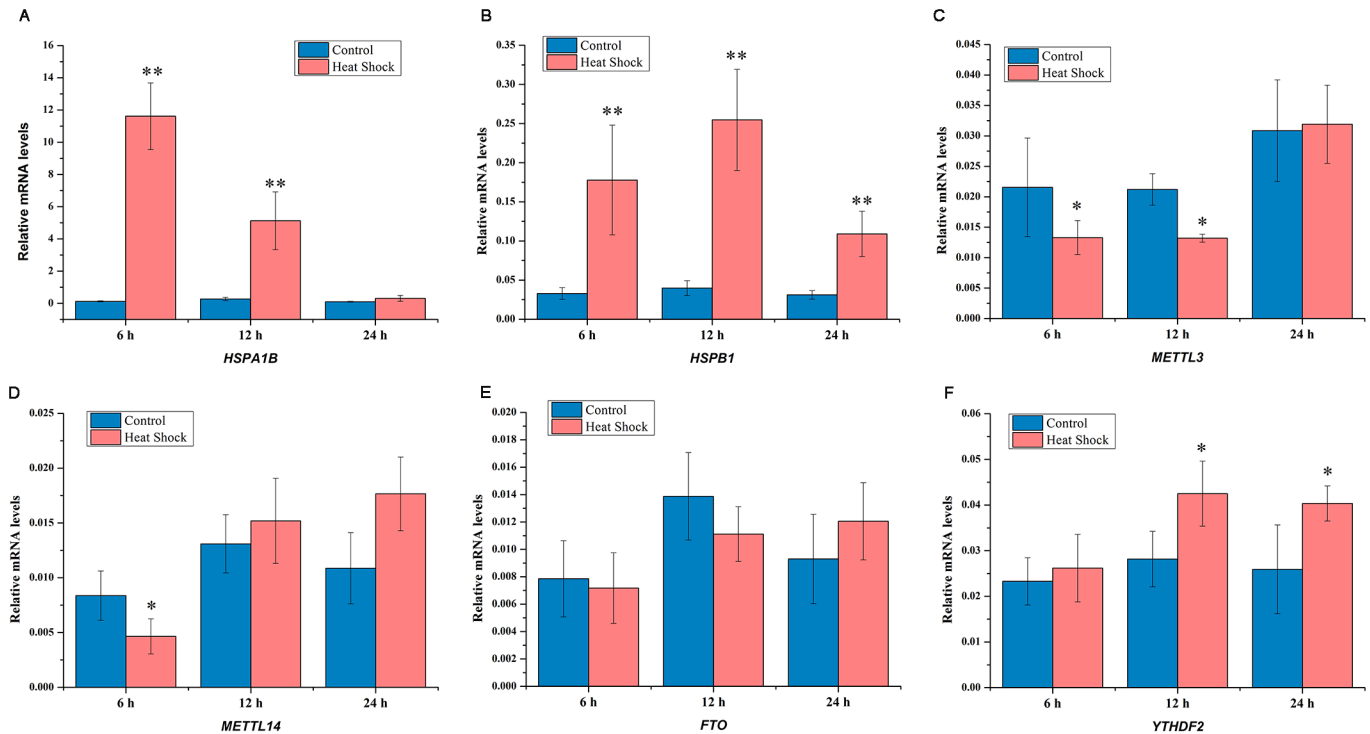
Fig 1. Effect of heat shock on *HSPs* and m⁶A mRNA methylation related genes. Expression of *HSPA1B* (*HSP70*) (**A**), *HSPB1* (*HSP27*) (**B**), *METTL3* (**C**), *METTL14* (**D**), *FTO* (**E**), and *YTHDF2* (**F**) mRNA at 6 h, 12 h, 24 h after heat shock in HepG2 cells. Data are shown as mean ± SEM (n = 3). *p value $\leq$ 0.05, **p value $\leq$ 0.01.

https://doi.org/10.1371/journal.pone.0198604.g001

heterodimer core complex of METTL3-METTL14 that functions in cellular m⁶A deposition on mammalian nuclear RNAs and the phenotypes of *METTL14* knockdown are the same with *METTL3*. In addition, it has been very well-described that METTL3 is m⁶A specific methyltransferases and regulates the levels of m⁶A [11]. Knockdown of METTL3 significantly decreased m⁶A methylation in many type of cell line and in vivo. Here, we did not confirm this. Our results shows that *METTL3* mRNA was decreased by 89% at 48 h after METTL3 knockdown in HepG2 cells ($p < 0.05$) (Fig 3A). The levels of METTL3 protein were also significantly decreased in HepG2 cells (Fig 3B). METTL3 knockdown in HepG2 cells significantly increased the expression of *HSP70* and *HSP27* mRNA compared to control ($p < 0.05$) (Fig 3C). In contrast, the levels of *HSP60* mRNA were inhibited following siMETTL3 treatment compared to the control ($p < 0.05$) (Fig 3C). There were no differences in abundance of *HSP90* and *HSF1* mRNA between control and siMETTL3 groups. In addition, knockdown of *METTL3* using a specific siRNA led to the decrease of relative cell viability in HepG2 cells determined by MTT (3-[4,5-dimethylthiazol-2-yl]-2, 5-diphenyl-tetrazolium bromide) at 24, 48, and 72 h after transfection without heat shock (Fig 3D). However, heat shock pretreatment attenuated the decrease of relative cell viability induced by knockdown of *METTL3* in HepG2 cells at 72 h (Fig 3D).

Knockdown of METTL3 does not change *HSPA1B* lifetime

The results of *HSPA1B* lifetime is shown in Fig 4A and 4B. The results showed that METTL3 knockdown in HepG2 cells did not affect the lifetime of *HSPA1B* compared to control.
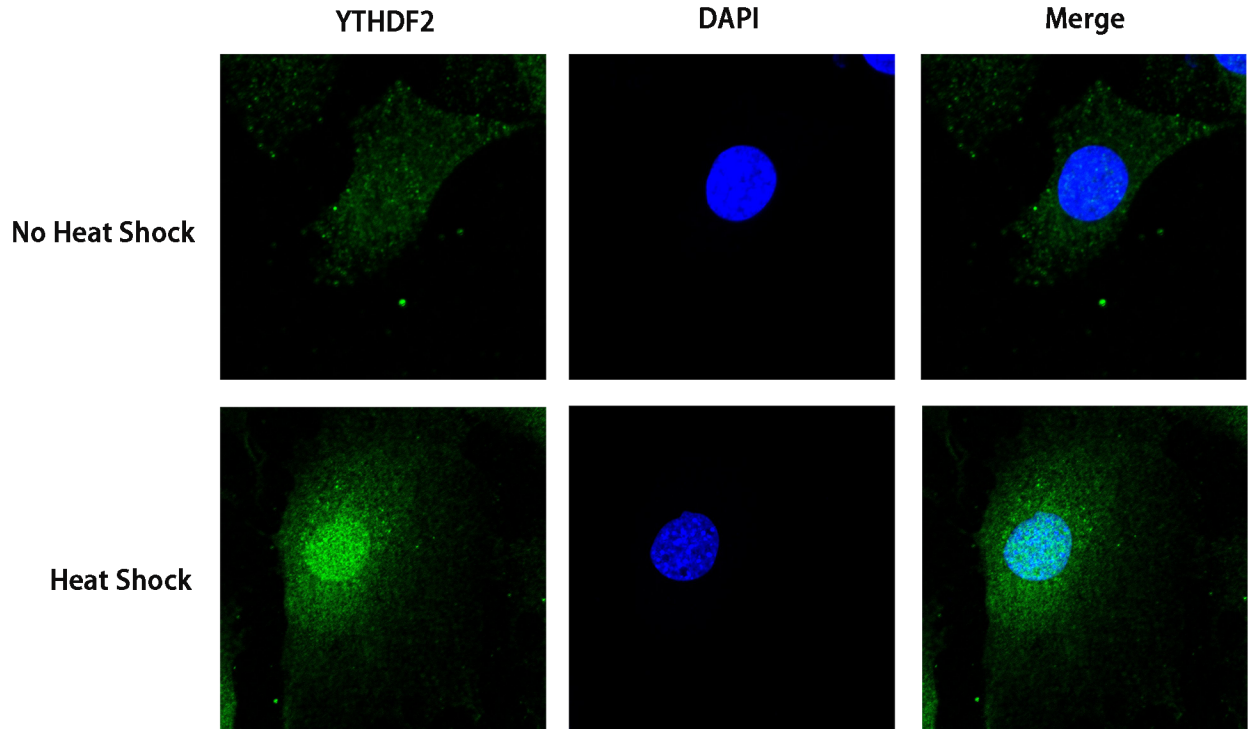
Fig 2. Localization of YTHDF2 under heat shock. The majority of YTHDF2 resided in the cytosol in normal conditions, whereas nearly all YTHDF2 translocated into the nucleus from the cytosol under heat shock stress. *Scale bar* = 88 μm.

https://doi.org/10.1371/journal.pone.0198604.g002

YTHDF2 knockdown affects HSPs expression and cell proliferation

In order to illuminate the function of m^{6}A binding protein, YTHDF2 was knockdowned in HepG2 cells. *YTHDF2* mRNA was decreased by 83% at 48 h after YTHDF2 knockdown in HepG2 cells ($p < 0.05$) (Fig 5A). Because YTHDF2 siRNA has been validated very well by our collaborator Dr. Chuan He, we did not further confirm the knockdown YTHDF2 using Western blot. The results showed that differences in *HSPA1B* and *HSPA9* mRNA expression were not observed between control and siYTHDF2 samples (Fig 5B). However, expression of *HSP90AA1*, *HSPD1*, and *HSPB1* mRNA were significantly increased by knockdown of YTHDF2 in HepG2 cells (Fig 5B and 5C). Furthermore, *YTHDF2* knockdown reduced the relative cell viability in HepG2 cells at 24, 48, and 72 h after transfection without heat shock (Fig 5D). Surprisingly, heat shock pretreatment increased the relative cell viability after knockdown of *YTHDF2* (Fig 5D).

Profile of HSPs gene-m^{6}A methylation

Using previously described methods for m^{6}A-seq [22], we sequenced the entire methylated RNA species purified from HepG2 cells. Coinciding with the previously reported pattern of m^{6}A peaks [11, 13], the m^{6}A sites of *HSPA1B*, *HSPB1*, *HSPA9*, *HSP90AA1*, *HSPD1*, *HSF1* transcripts mainly distribute on exons and around stop codons (Fig 6A–6F). In addition, *HSPA1B*, *HSPB1*, *HSPA9*, and *HSPD1* transcripts were found to have m^{6}A enrichments in both the 5'UTR and 3'UTR. M^{6}A enrichment for *HSP90AA1* transcript was found only in the 5'UTR (Fig 6D). In contrast, HSF1 transcript showed m^{6}A enrichments mainly in the 3'UTR (Fig 6F). Moreover, knockdown of *METTL3* changed methylation patterns of *HSPA1B*, *HSPA9*, *HSPB*1, and *HSPD1*.
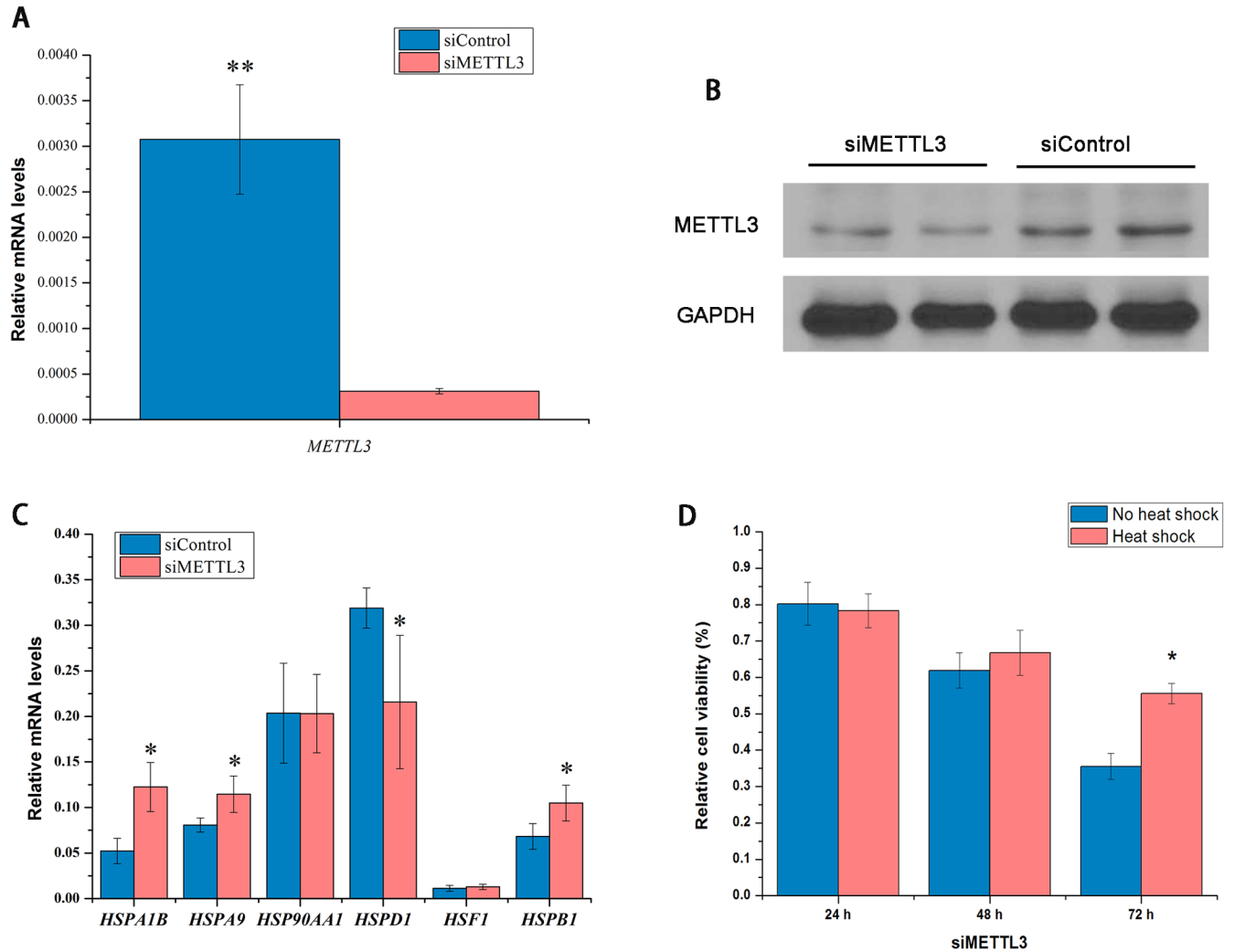
Fig 3. Effect of METTL3 knockdown on HSPs and cell viability in HepG2 cells. Expression of *METTL3* mRNA and protein in HepG2 cells after METTL3 knockdown (**A** and **B**). (n = 3). Expression of *HSPA1B* (*HSP70*), *HSPA9* (*HSP70*), *HSP90AA1* (*HSP90*), *HSPD1* (*HSP60*), *HSF1*, and *HSPB1* (*HSP27*) mRNA upon METTL3 knockdown in HepG2 cells (**C**) (n = 3). The relative cell viability determined by MTT at 24, 48, and 72 h post-transfection of METTL3 siRNA with or without heat shock pretreatment (**D**) (n = 6). Data are shown as mean ± SEM. *p value ≤ 0.05, **p value ≤ 0.01.

Discussion

As one of the most prevalent modifications in mRNAs, m⁶A methylation has emerged as a key post-transcriptional regulator of gene expression [23]. In the present study, we observed that METTL3 or YTHDF2 knockdown significantly changed HSPs gene expression, and heat shock induced nuclear localization of YTHDF2. M⁶A methylation peaks of HSPs are mainly enriched on exons and around stop codons. The precise mechanism for different expression of HSPs induced by m⁶A RNA methylation requires further investigation.

As a novel epitranscriptomic marker, m⁶A is a widespread modification present in over 7,000 human genes, including circadian genes [24], *p53* [15], *Notch1α* [25], and *XIST* [26] genes. Zhou et al. [21] also showed that although there was no effect on *HSP70* mRNA expression, YTHDF2 activated its mRNA translation under heat shock stress. However, the effect of m⁶A RNA methylation on other stress-inducible chaperone HSP90, HSP60, and HSP27 is still unknown. Here we found that heat shock treatment significantly increased *HSP70* mRNA
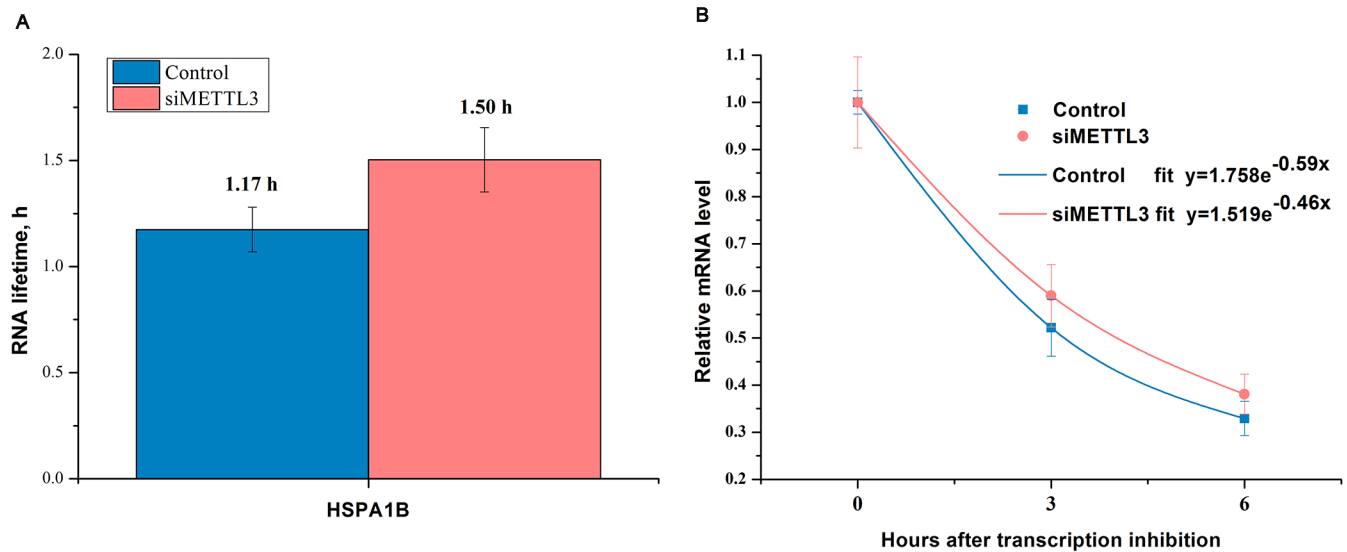
Fig 4. Effect of METTL3 knockdown on the lifetime of HSPA1B in HepG2 cells. Lifetime of *HSPA1B* (*HSP70*) mRNA in the samples following knockdown of *METTL3* in HepG2 cells (**A**). The relative mRNA levels of *HSPA1B* (*HSP70*) in the samples following knockdown of *METTL3* in HepG2 cells at 0 h, 3 h, and 6 h (**B**).

with a decrease in METTL3, whereas we observed an increase in YTHDF2, suggesting a dynamic m⁶A mRNA methylation response to environmental changes. In order to investigate whether these changes are associated with HSPs gene expression, we inhibited METTL3 in HepG2 cells using siRNA. We found that *HSPA1B*, *HSPA9*, and *HSP60* mRNA showed significant changes, but no differences were observed for *HSP90AA1* and *HSF1* mRNA. These different effects may be associated with different m⁶A site and abundance on HSPs transcript. Since m⁶A RNA methylation contributes to mRNA stability, we performed HSP70 lifetime analysis in HepG2 cells and found that METTL3 knockdown did not change HSP70 mRNA lifetime, suggesting that it may have other regulatory mechanisms of m⁶A on HSPs.

M⁶A is recognized by the YTH domain family proteins [27]. There are five proteins (YTHDF1-3, YTHDC1, and YTHDC2) that contain the YTH domain in human cells. YTHDF1-3 are primarily cytoplasmic, whereas YTHDC1 is located primarily in the nucleus [13, 27]. YTHDF1 binds m⁶A-modified mRNAs through interactions with initiation factors and ribosomes to increase translational output [28]. YTHDF2 regulates mRNA decay by binding to m⁶A transcripts, which results in their re-localization from the pool of ribosome-associated translatable transcripts to cellular RNA decay sites such as P-bodies [13]. In the present study, YTHDF2 knockdown did not change *HSPA1B*, *HSPA9* mRNA expression, but significantly increased *HSP90AA1*, *HSPD1*, and *HSPB1* mRNA expression. Altered expression of HSPs may be associated with YTHDF2 function, which depends on the m⁶A site of the target gene. Immunofluorescence staining showed that the majority of YTHDF2 was present in the cytosol, however, nearly all YTHDF2 translocated from the cytosol into the nucleus under heat shock, further confirming that YTHDF2 regulates HSPs mRNA expression.

Different sites and abundance of m⁶A on transcript may lead to altered gene output. In addition, the function of YTHDF2 may depend on the cellular context and the m⁶A site of the target gene. A previous study showed that YTHDF2 knockdown increased the m⁶A/A ratio and the stabilization of the RNA targets [13]. However, upon heat shock stress, the nuclear YTHDF2 protects the 5'UTR of stress-induced transcripts from demethylation and activates
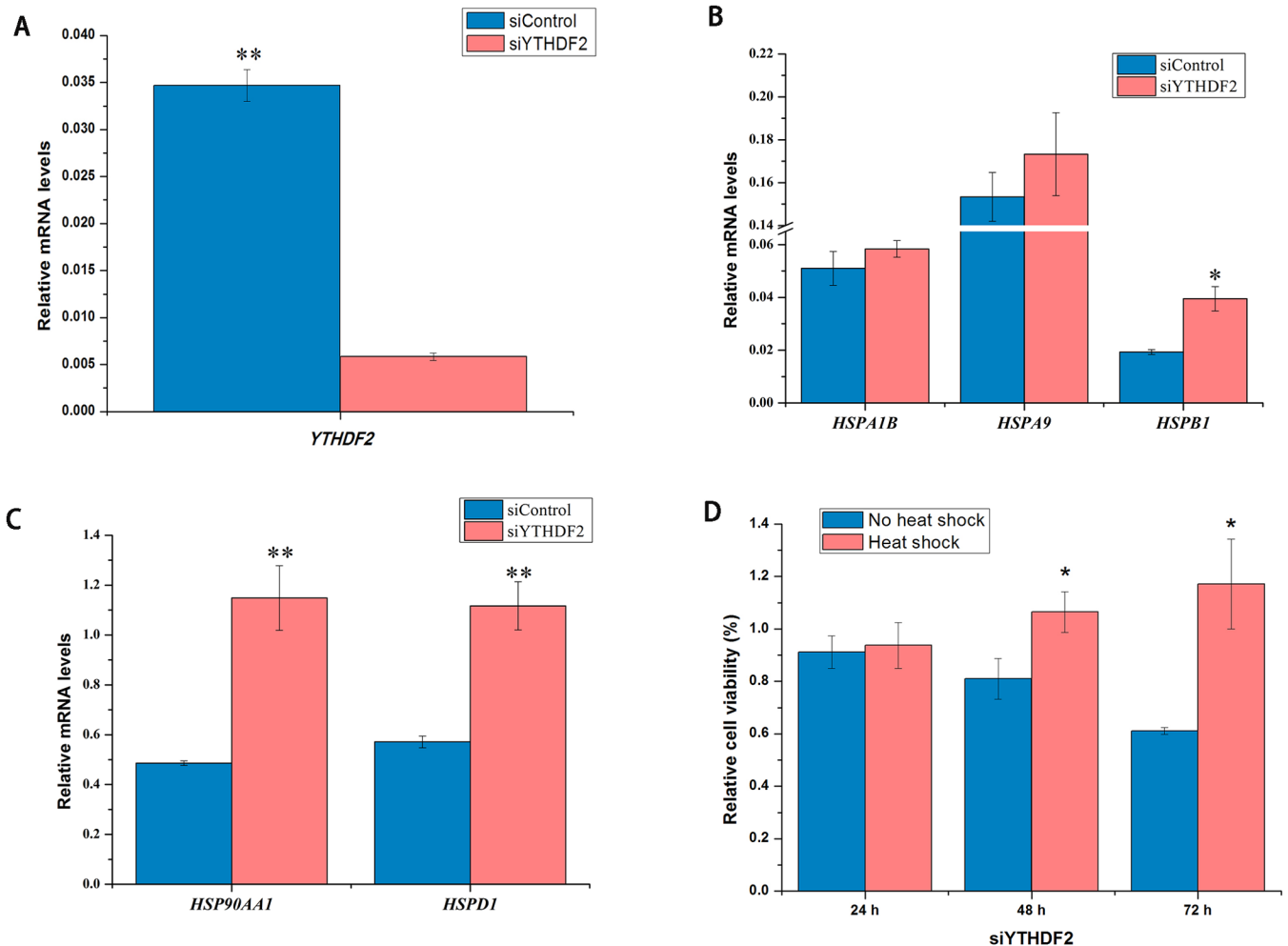
Fig 5. Effect of YTHDF2 on HSPs mRNA expression and cell viability in HepG2 cells. YTHDF2 knockdown decreased YTHDF2 mRNA in HepG2 cells (**A**). Expression of *HSPA1B* (*HSP70*), *HSPA9* (*HSP70*), *HSPB1* (*HSP27*), *HSP90AA1* (*HSP90*), *HSPD1* (*HSP60*) mRNA from the sample of YTHDF2 knockdown in HepG2 cells (**B** and **C**). The relative cell viability determined by MTT at 24, 48, and 72 h after knockdown of YTHDF2 with or without heat shock pretreatment (**D**) (n = 6). Data are shown as mean ± SEM. *p value ≤ 0.05, **p value ≤ 0.01.

translation [21]. Using m⁶A-seq, we dissected the profile of HSPs RNA methylation and found that there are different distribution characteristic of m⁶A between HSPs transcript. We also observed changes of methylation patterns of HSPs mRNA after *METTL3* knockdown. These results, to some extent, suggest that different expression of *HSP70*, *HPS90*, *HSP60*, and *HSP27* are modulated by METTL3 or YTHDF2 knockdown in HepG2 cells *in vitro*.

M⁶A modification on gene expression impacts a variety of physiological events, including mammalian embryonic stem cell fate [29], X chromosome inactivation [26], zebrafish maternal-to-zygotic transition [16], haematopoietic stem and progenitor cell specification [25], metabolic diseases, and the stability of the mammalian circadian clock [24]. In the present study, we also observed that decrease of m⁶A RNA methylation reduces cell viability in HepG2 cells. However, heat shock pretreatment attenuated the decrease of cell viability induced by knockdown of *METTL3* or *YTHDF2* in HepG2 cells. Further investigation is needed to reveal the underlying mechanism of these changes.
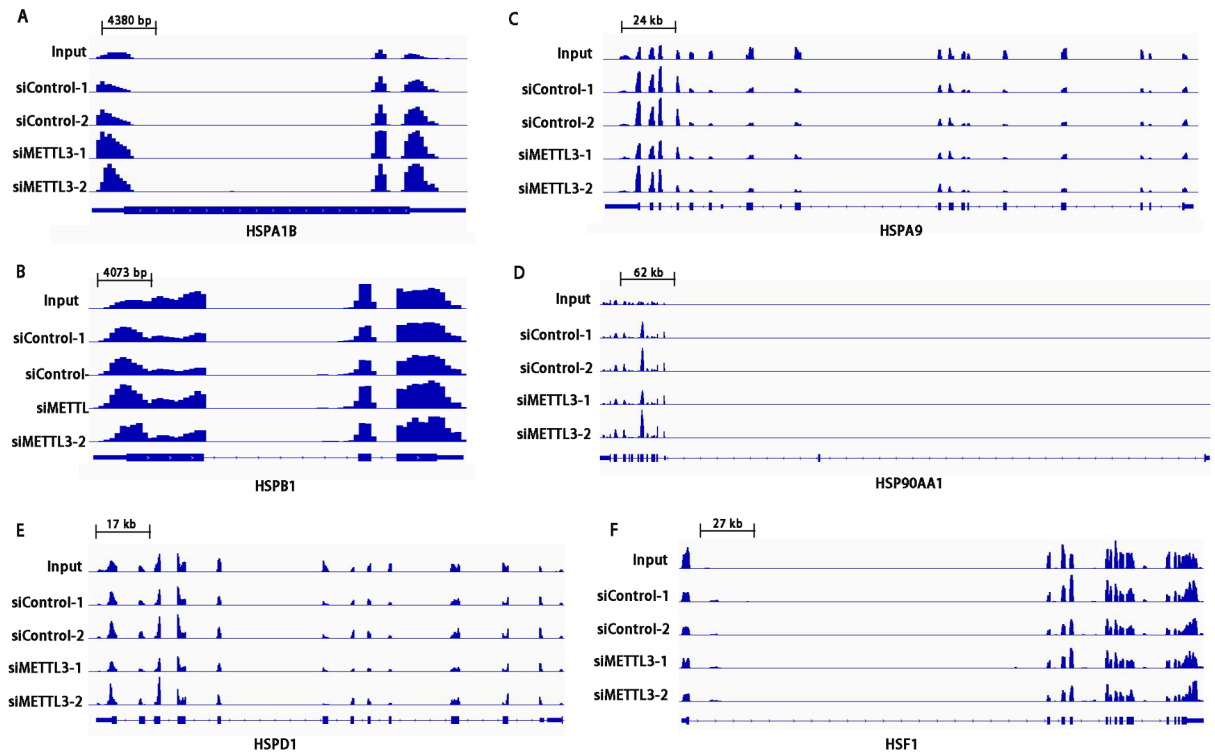
Fig 6. M⁶A methylated peaks of HSPs mRNA. Integrative genomics viewer (IGV) plots showing m⁶A methylated peaks for *HSPA1B* (*HSP70*) (**A**), *HSPB1* (*HSP27*) (**B**), *HSPA9* (*HSP70*) (**C**), *HSP90AA1* (*HSP90*) (**D**), *HSPD1* (*HSP60*) (**E**), *HSF1* (**F**) mRNA in HepG2 cells. Blue boxes represent exons and blue lines represent introns. *n* = 2.

https://doi.org/10.1371/journal.pone.0198604.g006

In conclusion, the expression of HSPs is modulated by m⁶A RNA methylation. This finding would provide insights into the new regulatory mechanisms of HSPs in normal and stress situations.

Acknowledgments

Author Contributions

Conceptualization: Xiang Zhong.

Data curation: Tian Wang, Xiang Zhong.

Formal analysis: Xiang Zhong.

Funding acquisition: Xiang Zhong.

Investigation: Jiayao Yu, Yi Li, Xiang Zhong.

Methodology: Xiang Zhong.

Project administration: Xiang Zhong.

Resources: Xiang Zhong.

Software: Xiang Zhong.

Supervision: Xiang Zhong.

Validation: Xiang Zhong.

Visualization: Xiang Zhong.

Writing – original draft: Xiang Zhong.

Writing – review & editing: Tian Wang, Xiang Zhong.

References

1. Oellmy R, Boellmann F. Chaperone regulation of the heat shock protein response. Molecular Aspects of the Stress Response: Chaperones, Membranes and Networks: Springer; 2007. p. 89–99.

2. Zhong X, Li W, Huang X, Zhang L, Yimamu M, Raiput N, et al. Impairment of cellular immunity is associated with overexpression of heat shock protein 70 in neonatal pigs with intrauterine growth retardation. Cell Stress Chaperones. 2012; 17(4):495–505. https://doi.org/10.1007/s12192-012-0326-6 PMID: 22270614

3. Zhong X, Wang T, Zhang X, Li W. Heat shock protein 70 is upregulated in the intestine of intrauterine growth retardation piglets. Cell Stress Chaperones. 2010; 15(3):335–42. https://doi.org/10.1007/s12192-009-0148-3 PMID: 19830596

4. Kampinga HH, Hageman J, Vos MJ, Kubota H, Tanguay RM, Bruford EA, et al. Guidelines for the nomenclature of the human heat shock proteins. Cell Stress Chaperones. 2009; 14(1):105–11. https://doi.org/10.1007/s12192-008-0068-7 PMID: 18663603

5. Ciocca DR, Arrigo AP, Calderwood SK. Heat shock proteins and heat shock factor 1 in carcinogenesis and tumor development: an update. Arch Toxicol. 2013; 87(1):19–48. https://doi.org/10.1007/s00204-012-0918-z PMID: 22885793

6. Smith ST, Petruk S, Sedkov Y, Cho E, Tillib S, Canaani E, et al. Modulation of heat shock gene expression by the TAC1 chromatin-modifying complex. Nat Cell Biol. 2004; 6(2):162. https://doi.org/10.1038/ncb1088 PMID: 14730313

7. Miozzo F, Sabéran-Djoneidi D, Mezger V. HSFs, stress sensors and sculptors of transcription compartments and epigenetic landscapes. J Mol Biol. 2015; 427(24):3793–816. https://doi.org/10.1016/j.jmb.2015.10.007 PMID: 26482101

8. Marinova Z, Leng Y, Leeds P, Chuang D-M. Histone deacetylase inhibition alters histone methylation associated with heat shock protein 70 promoter modifications in astrocytes and neurons. Neuropharmacology. 2011; 60(7):1109–15.

9. Fritah S, Col E, Boyault C, Govin J, Sadoul K, Chiocca S, et al. Heat-shock factor 1 controls genome-wide acetylation in heat-shocked cells. Mol Biol Cell. 2009; 20(23):4976–84. https://doi.org/10.1091/mbc.E09-04-0295 PMID: 19793920

10. Wei C-M, Gershowitz A, Moss B. Methylated nucleotides block 5′ terminus of HeLa cell messenger RNA. Cell. 1975; 4(4):379–86. PMID: 164293

11. Liu J, Yue Y, Han D, Wang X, Fu Y, Zhang L, et al. A METTL3-METTL14 complex mediates mammalian nuclear RNA N⁶-adenosine methylation. Nat Chem Biol. 2014; 10(2):93–5. https://doi.org/10.1038/nchembio.1432 PMID: 24316715

12. Jia G, Fu Y, Zhao X, Dai Q, Zheng G, Yang Y, et al. N⁶-methyladenosine in nuclear RNA is a major substrate of the obesity-associated FTO. Nat Chem Biol. 2011; 7(12):885–7. https://doi.org/10.1038/nchembio.687 PMID: 22002720

13. Wang X, Lu Z, Gomez A, Hon GC, Yue Y, Han D, et al. N⁶-methyladenosine-dependent regulation of messenger RNA stability. Nature. 2014; 505(7481):117–20. https://doi.org/10.1038/nature12730 PMID: 24284625

14. Wang X, He C. Reading RNA methylation codes through methyl-specific binding proteins. RNA Biol. 2014; 11(6):669–72. https://doi.org/10.4161/rna.28829 PMID: 24823649

15. Dominissini D, Moshitch-Moshkovitz S, Schwartz S, Salmon-Divon M, Ungar L, Osenberg S, et al. Topology of the human and mouse m⁶A RNA methylomes revealed by m⁶A-seq. Nature. 2012; 485(7397):201–6. https://doi.org/10.1038/nature11112 PMID: 22575960

16. Zhao BS, Wang X, Beadell AV, Lu Z, Shi H, Kuuspalu A, et al. m⁶A-dependent maternal mRNA clearance facilitates zebrafish maternal-to-zygotic transition. Nature. 2017; 542(7642):475. https://doi.org/10.1038/nature21355 PMID: 28192787

17. Xiao W, Adhikari S, Dahal U, Chen Y-S, Hao Y-J, Sun B-F, et al. Nuclear m 6 A reader YTHDC1 regulates mRNA splicing. Mol Cell. 2016; 61(4):507–19. PMID: 26876937

18. Zheng G, Dahl JA, Niu Y, Fedorcsak P, Huang C-M, Li CJ, et al. ALKBH5 is a mammalian RNA demethylase that impacts RNA metabolism and mouse fertility. Mol Cell. 2013; 49(1):18–29. https://doi.org/10.1016/j.molcel.2012.10.015 PMID: 23177736

19. Meyer KD, Patil DP, Zhou J, Zinoviev A, Skabkin MA, Elemento O, et al. 5′ UTR m⁶A promotes cap-independent translation. Cell. 2015; 163(4):999–1010. https://doi.org/10.1016/j.cell.2015.10.012 PMID: 26593424

20. Xiang Y, Laurent B, Hsu C-H, Nachtergaele S, Lu Z, Sheng W, et al. RNA m⁶A methylation regulates the ultraviolet-induced DNA damage response. Nature. 2017; 543:573–6. https://doi.org/10.1038/nature21671 PMID: 28297716

21. Zhou J, Wan J, Gao X, Zhang X, Qian S-B. Dynamic m⁶A mRNA methylation directs translational control of heat shock response. Nature. 2015; 526(7574):591. https://doi.org/10.1038/nature15377 PMID: 26458103

22. Dominissini D, Moshitch-Moshkovitz S, Salmon-Divon M, Amariglio N, Rechavi G. Transcriptome-wide mapping of N⁶-methyladenosine by m⁶A-seq based on immunocapturing and massively parallel sequencing. Nat Protoc. 2013; 8(1):176–89. https://doi.org/10.1038/nprot.2012.148 PMID: 23288318

23. Fu Y, Dominissini D, Rechavi G, He C. Gene expression regulation mediated through reversible m⁶A RNA methylation. Nature reviews Genetics. 2014; 15(5):293. https://doi.org/10.1038/nrg3724 PMID: 24662220

24. Fustin J-M, Doi M, Yamaguchi Y, Hida H, Nishimura S, Yoshida M, et al. RNA-methylation-dependent RNA processing controls the speed of the circadian clock. Cell. 2013; 155(4):793–806. https://doi.org/10.1016/j.cell.2013.10.026 PMID: 24209618

25. Zhang C, Chen Y, Sun B, Wang L, Yang Y, Ma D, et al. m⁶A modulates haematopoietic stem and progenitor cell specification. Nature. 2017; 549(7671):273–6. https://doi.org/10.1038/nature23883 PMID: 28869969

26. Patil DP, Chen C-K, Pickering BF, Chow A, Jackson C, Guttman M, et al. m⁶A RNA methylation promotes XIST-mediated transcriptional repression. Nature. 2016; 537(7620):369. https://doi.org/10.1038/nature19342 PMID: 27602518

27. Xu C, Wang X, Liu K, Roundtree IA, Tempel W, Li Y, et al. Structural basis for selective binding of m⁶A RNA by the YTHDC1 YTH domain. Nat Chem Biol. 2014; 10(11):927–9. https://doi.org/10.1038/nchembio.1654 PMID: 25242552

28. Wang X, Zhao BS, Roundtree IA, Lu Z, Han D, Ma H, et al. N⁶-methyladenosine modulates messenger RNA translation efficiency. Cell. 2015; 161(6):1388–99. https://doi.org/10.1016/j.cell.2015.05.014 PMID: 26046440

29. Batista PJ, Molinie B, Wang J, Qu K, Zhang J, Li L, et al. m⁶A RNA modification controls cell fate transition in mammalian embryonic stem cells. Cell stem cell. 2014; 15(6):707–19. https://doi.org/10.1016/j.stem.2014.09.019 PMID: 25456834